Evaluating Opportunities for Broad-Scale Remote Sensing of TSS on Small Rivers

Rebecca M. Diehl, Research Assistant Professor, Department of Geography and Geosciences, University of Vermont, Burlington, VT, Rebecca.Diehl@uvm.edu
Kristen L. Underwood, Research Assistant Professor, Department of Civil and Environmental Engineering, University of Vermont, Burlington, VT, Kristen.Underwood@uvm.edu
Robert Watt, Research Assistant, University of Vermont, Burlington, VT, robertbuiswatt@gmail.com
Scott D. Hamshaw, Adjunct Assistant Professor, Department of Civil and Environmental Engineering, University of Vermont, Burlington, VT, Scott.Hamshaw@uvm.edu
Nima Pahlevan, Research Scientist SME, Science Systems and Applications, Inc, NASA Goddard Space Flight Center, University of Maryland, Department of Geography, nima.pahlevan@nasa.gov

Abstract

Although broad-scale remote sensing applications are increasingly being adopted into water quality assessments, the feasibility of such applications on smaller rivers (< 150 m. width) is not well understood. We evaluated the application of widely used single band and multi-conditional Total Suspended Solid (TSS) algorithms within the relatively small rivers of the Lake Champlain Basin in the Northeastern US. We identified Sentinel-2 images captured within a few hours of depth-integrated TSS samples measured in 10 tributaries (17 to 117 m wide) and corrected them for atmospheric conditions. Errors in the relationship between measured and predicted TSS values were used to explore potential limits on the application of existing TSS algorithms to small rivers. We found that there are settings along smaller rivers, and flow and seasonal conditions, under which broad scale remote sensing applications may be applicable. Remote sensing algorithms had greatest success predicting TSS when flow depths were sufficiently deep (approximately greater than 80-90 cm), biological activity was limited (as measured by temperature) and on rivers with a relatively fine-grained sediment load (i.e., potentially wash-load dominated). We hypothesized that algorithm performance on smaller rivers would be prone to larger errors due to the greater influence of contrasting reflectance signals from soils and vegetation along river banks. The degree of limitation from this adjacency effect was not evident in our dataset but may be because of the correlation between river size and the character of the transported sediment, which had a significant impact on TSS errors. Our results highlight the feasibility of extending remote sensing applications to smaller river networks in temperate regions, especially for certain geologic settings and during the colder months, when in-situ monitoring is particularly challenging.

Introduction

Increasing intensity of landscape change and a warming climate have enhanced the occurrence of harmful algal blooms and overall degradation of riverine water quality (Foley et al., 2005; Murray et al., 2022). Targeting source areas of sediment and pollutants can help meet water quality goals and increase overall ecosystem health (Fleming et al., 2022). Broad-scale remote sensing-based analyses have been used to identify the source, distribution, and temporal

patterns of river-transported constituents (Gardner et al., 2021) and represent an improvement over financially and logistically challenging in-situ data collection programs (Stanley et al., 2019). But remote sensing approaches for riverine water quality applications have been mostly tested on large rivers (> 150 m in width; e.g., Dethier et al., 2019), limiting our understanding of the applicability to smaller watersheds. Smaller rivers represent most of the river network (Downing et al., 2012) and are sites of important biogeochemical and physical processes (Alexander et al., 2007; Scott et al., 2019; Wohl, 2017).

Predicting water quality parameters, specifically total suspended solids (TSS), often relies on a simple relationship between surface reflectance and the concentration of suspended solids, which tend to reflect incoming electromagnetic radiation rather than absorb it like water. Application of TSS algorithms in inland water can be challenging (Pahlevan et al., 2021), and additional challenges exist in fluvial settings because of narrower, shallow water bodies with spatially and temporally variable, and optically complex water properties (Olmanson et al., 2013; Topp et al., 2020). In near-bank areas, edge effects of adjacent terrestrial features can significantly disturb the water-leaving radiance signal (Zhao et al., 2014). Vegetation overlying the riverbank and leaves on riparian trees may further complicate reflectance, as does the signal from the channel bed if river flows are too shallow, or water is too clear (Volpe et al., 2011).

River water and suspended sediment characteristics that influence river optical properties can also impact the accuracy of estimated water quality parameters (Kilham et al., 2012). Coarser grained sediment loads and those with a low mass fraction of fine-grained particles can lead to model underestimation of total suspended solids, and differences in the minerology can lead to inter-river and intra-river variation in regression models (Novo et al., 1989). Water-transported organic matter also introduces variability in river reflectance. Notably, chlorophyll-a generally absorbs blue and red light and reflects near infrared (NIR). Reflectance in these spectra is also associated with high suspended sediment concentrations, potentially leading to incorrect TSS estimations (Martinez et al., 2015a). Vertical distribution of suspended sediments in the water column can also be highly variable depending on the flow dynamics and sediment grain sizes (Armijos et al., 2017). Transport of finer particles often occurs higher in the water column, potentially as wash-load, compared to coarser particles, which remain closer to the bed and thus may be hard to detect at the surface (Bi et al., 2011). And the distribution of particle sizes is highly variable across a river, from one river to another, and over time, as finer particles are often flushed downstream during the early parts of a flood (Landers & Sturm, 2013). Such variability can reduce prediction accuracy, especially because of the different sampling techniques (i.e., surface vs depth-integrated) used in the creation of calibration data (Dethier et al., 2019).

In this paper we explored the feasibility of using broad-scale remote sensing products to predict the concentration of total suspended solids (TSS) on smaller rivers, defined as those narrower than 150 meters but wider than the image resolution (i.e., 10 m). We built a dataset of observed in-situ TSS samples collected on 10 smaller rivers (17 to 117 m wide) in the Lake Champlain Basin of the northeastern United States and matched these observations with nearest-in-time available European Space Agency's Sentinel-2 multi-spectral imagery. We evaluated which factors describe the difference between estimated (from widely used TSS algorithms) and observed TSS values to better constrain uncertainties and guide future development of remote sensing applications further up the river network.

Based on our understanding of the factors that may limit application of broad-scale remote sensing to smaller rivers, we hypothesized that errors in estimated TSS may be described by:

(1) Watershed Setting factors that may determine channel dimensions (width and depth) and the character of the transported load. We expected that narrower rivers and those with coarser sediment loads will have greater errors because of the adjacency effect of channel banks and the uncertainty introduced with depth-integrated observed TSS samples (see Methods).

(2) Flow Conditions including discharge and associated flow depth, and the portion of the hydrograph sampled. We expected that shallower flow depths and samples collected on the falling limb or during steady flows will have greater uncertainties, because of the impact of backscattering and the potential for reduced presence of fines in the water column.

(3) Seasonal Influences including the growing season and the presence of organic material. We expected that errors will be smaller outside of the growing season, when deciduous riparian trees do not have leaves, herbaceous vegetation has senesced, and biological activity is suppressed.

Study Area and Methods

Tributaries of the Lake Champlain Basin

This study focused on the major tributaries to Lake Champlain in New York and Vermont (Figure 1), which are monitored as part of the Lake Champlain Long Term Monitoring Project (LTMP) (NY State DEC & VT DEC, 2021). Excess phosphorus has impaired the water quality of Lake Champlain, prompting the development of a Total Maximum Daily Load (TMDL) for Vermont and New York, and motivating the states to track phosphorus, sediment, and other indicators of overall ecosystem health (Smeltzer et al., 2012). Under a full range of flow conditions, the LTMP samples as many as 21 tributary stations twelve or more times per year, generally co-locating sampling with USGS stream gages. Depth-integrated Total Suspended Sediment (TSS) samples are obtained either using a DH-48 or DH-59 (NY State DEC & VT DEC, 2020).

Previous glaciation in the Lake Champlain Basin contributes to the distinct geography of its tributary watersheds, influencing the nature of sediment and particulate phosphorus (PP) sourcing and transport (Medalie, 2014; Underwood et al., 2017). For eighteen of the 21 LTMP tributaries with greater than 25 years of monitoring, Underwood et al (2017) evaluated catchment characteristics associated with flow-normalized mean annual sediment and nutrient concentration and flux. Watersheds with relatively high mean annual fluxes of TSS and PP are characterized by higher-than-average basin relief and mean annual precipitation (MAP). This contrasts with watersheds of lower annual fluxes that are typically smaller in area, have less relief, and lower-than-average MAP. Yet, lower-flux basins also have higher baseline supplies of TSS and PP as a result of the predominance of glaciolacustrine soils and sediments they flow through, that are dominated by silts and clays, and therefore easily transported over a larger range of flows (Underwood et al., 2017). They also have higher mean annual concentrations of PP and TSS than their high-annual-flux counterparts (Medalie, 2014; Underwood et al., 2017). LTMP tributaries range in size from 137 to 2,753 km^2 and river channel widths at the outlets to Lake Champlain are less than 150 m.

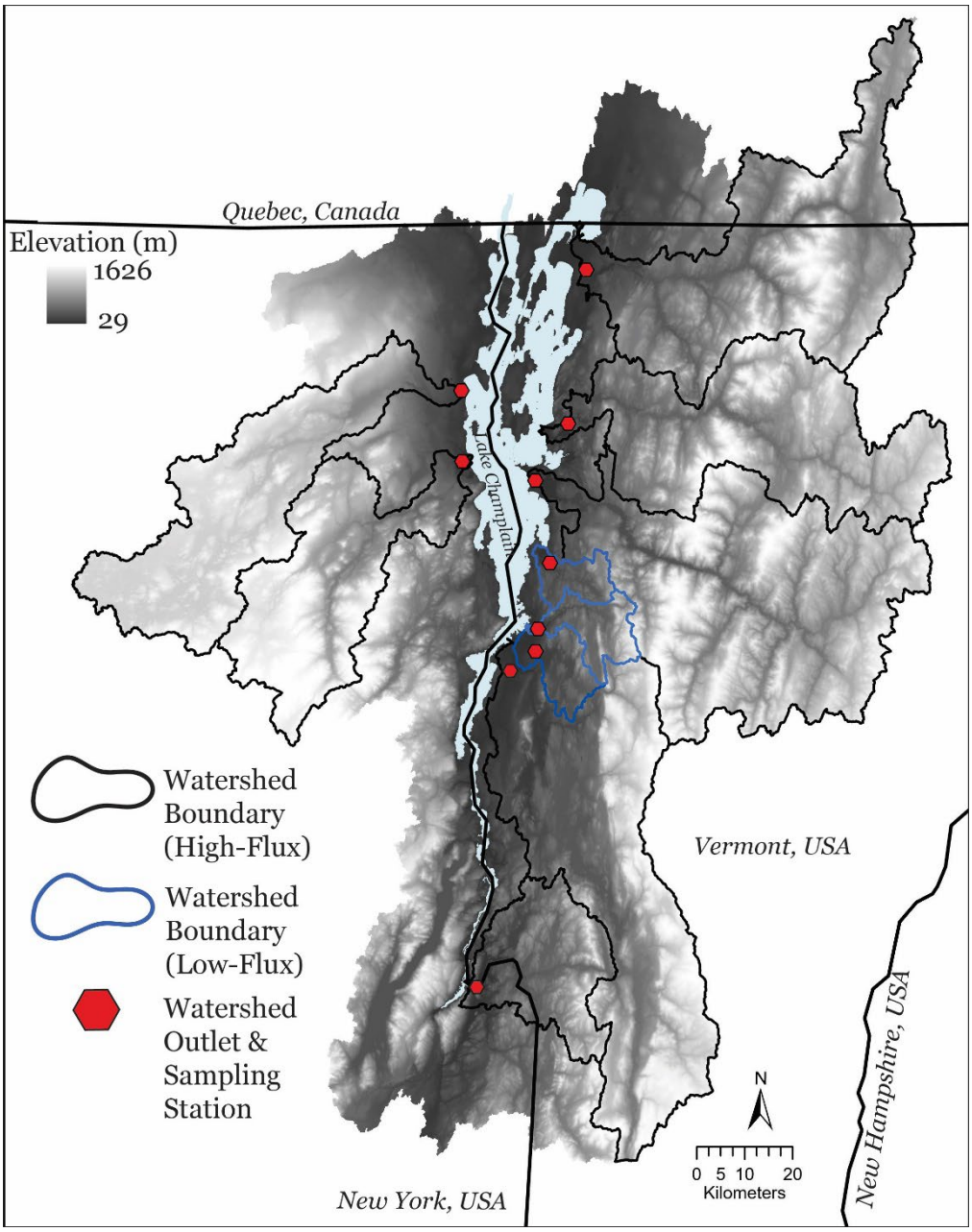

Figure 1. Ten major tributaries to the Lake Champlain Basin in Vermont and New York used in this study that are monitored for TSS and their outlets monitored for TSS in the Lake Champlain Basin in Vermont and New York, USA

Dataset Development

For ten of the monitored tributaries (Figure 1), we identified matched pairs of TSS sampling events and cloud-free scenes collected within 5 hours by the Multispectral Instrument (13 bands) on board the European Space Agency's Sentinel-2. We clipped each scene to the matched sampling location and processed the clipped images in ACOLITE (version 20211124.0), an open-source software platform designed specifically for atmospheric correction over marine and inland waters (Vanhellemont & Ruddick, 2016). Using the default dark spectrum fitting method, we calculated the remote sensing reflectance (*Rrs*) for the four 10-meter bands (red, green, blue, NIR). We estimated TSS as a function of *Rrs* from two widely used algorithms

developed for open and coastal waters: the single-band "*Nechad*" (Nechad et al., 2010), calculated directly in ACOLITE, using *Rrs* 665 nm, and the multi-conditional "*Novoa*" (Novoa et al., 2017). We note that while *Novoa* was developed using Sentinel B8a (narrow NIR), which is 20-m, we used the 10-m Sentinel B8 (NIR). Expected TSS values from *Nechad* and *Novoa* were extracted for the pixels within the river around the sampling point, removing "mixed" river-land pixels from the averaging as best we could.

As a result, we developed a matched dataset of observed and estimated TSS values. We classified each entry based on six factors that generally describe the watershed setting, flow conditions, and seasonal influences (Table 1), which we hypothesized may explain the variability between observed and estimated TSS values and highlight opportunities (and limitations) for remote sensing of TSS in small rivers.

Table 1. Definition of the six factors, grouped by watershed setting, flow condition, or seasonal influence hypothesized to describe errors in estimated TSS values

	Factor	Category 1	Definition	Category 2	Definition
Watershed Setting	Channel Width	Narrow	bankfull channel < 50 meters	Wide	bankfull channel ≥ 50 meters
	River Flux*	High Flux	TSS and PP clusters 1 and 3 in Underwood et al (2017)	Low Flux	TSS and PP cluster 2 in Underwood et al. (2017)
Flow Condition	Flow Depth	Shallow	less than modeled threshold for visible beds, based on observed TSS**	Deep	more than modeled threshold for visible beds, based on observed TSS**
	Hydrograph	Rising Limb	increasing discharge as measured at the nearest gage	Recession/ Flat	a decrease, or no change, to discharge as measured at the nearest gage
Seasonal Influence	Vegetation	Leaf Off	October 16 to April 30	Leaf on	May 1 to October 15
	Water Temperature	Cold	water temperature < 15°C	Warm	water temperature ≥15°C

* as determined by the total annual flux

**based on radiative transfer modeling by Legleiter et al (2011)

Watershed Setting: Channel width varies systematically through a watershed, with increasing discharge, but is also more locally a function of the boundary materials, gradient, and the character of the vegetation that lines the banks, and has been used as an indicator of, or filter for, the use of remote sensing for monitoring water quality (Dethier et al., 2019). To evaluate the importance of channel width above a minimum threshold (i.e., greater than the resolution of the images used), we measured channel width from top of bank to top of bank using information in aerial photographs and LiDAR-derived DEMs, as transition in vegetation and change in land surface slope. We classified the tributaries into two classes (<50-m wide and ≥50-m wide), based on the rule of thumb that the channel should be 5-times the multi-spectral imagery resolution, or 50-m for this study. We also classified the tributaries by their expected annual TSS fluxes based on the classification of Underwood et al. (2017). Because low-flux rivers in the region also have high background levels of turbidity, potentially indicative of a greater proportion of their load transported as washload, we expected that the relationship between reflectance and TSS would differ for low- versus high-flux rivers.

Flow Conditions: We assigned a flow depth at the time of image collection, based on an assumption that the stage at the nearby USGS streamflow gage approximated the average water column depth at the sampling point. We acknowledge that this is not a perfect assumption, as

flow depths have high spatial variability, but does provide bounds on the temporal variability of flows. We classified flow depths as either likely or unlikely to generate backscatter from the channel bed that would influence reflectance based on results from radiative transfer modeling by Legleiter et al. (2011). This model identified the maximum depth at which a sand bed is distinguishable from an infinitely deep water column, for increasing suspended sediment concentrations. Additionally, because the character of transported sediment often varies through a hydrograph (Landers & Sturm, 2013), we classified each of the dataset entries based on if they were collected on the rising limb or not (i.e., on the recession of the flood or during steady flows).

Seasonal Influences: To capture seasonal variability in biological activity, organic matter prevalence, and the potential for edge-effect interference of vegetation, we classified each sampling event as either occurring during leaf on (May 1 to October 15) or leaf off (October 16 to April 30) conditions. We also identified dataset entries that were likely to have larger chlorophyll-a (*chla*) concentrations. Because *chla* is no longer measured as part of the long-term monitoring project (as of 2005;NY State DEC & VT DEC, 2022) we used stream temperature as a proxy. From a t-test analysis of historical data at the long-term monitoring sites, we determined that stream temperatures greater than 15 degrees C are associated with higher *chla* concentrations (mean=2.9, SD=2.1), than stream temperatures below 15 degrees C (mean =4.0, SD=4.1; t(265)=-2.2, p=0.03).

Model and Dataset Evaluation

Two metrics were calculated following Pahlevan et al. (2022) and Smith et al. (2021) for the two algorithms (*Nechad* and *Novoa*) to gauge their performance. The median symmetric accuracy (ε) can be interpreted as a symmetric percentage error, equally penalizing over- and under-estimation. Perfect accuracy would have a sigma of 0%. Signed systematic percentage bias (β) also maintains symmetry, with positive values indicating over-estimation and negative indicating under-estimation. We calculated the accuracy and bias as follows:

$$\varepsilon = 100 \times \left(e^{median(|\log(e/o)|)} - 1\right)$$

$$MR = median(\log(e/o))$$

$$\beta = 100 \times sign(MR) \times \left(e^{|MR|} - 1\right)$$

where e and o stand for estimated and in-situ observed TSS values, respectively, and MR is the median ratio.

To understand how the difference (in % error) between observed and estimated TSS values is influenced by the sampling location's watershed setting, the flow conditions, and the seasonal characteristics, we compared means for groupings of metrics using one-way Analysis of Variance (ANOVA) methods followed by Tukey Honest Significant Difference (HSD) tests between individual group means. If the response variables were not normally distributed, based on the Shapiro-Wilks method, the nonparametric Kruskal-Wallis method was used and a post-hoc Dunn's Test (with a Bonferroni correction). We compared means between the six factors individually, and for all pairings of non-associated factors. Cramer's V test was used to test the strength of associations between the metrics. All analyses were performed in R v.4.2.2 (R Core Team, 2022) using the stats and FSA packages (Ogle et al., 2022).

Results

Twenty-one scenes were matched with sampling dates from one or more of the ten tributaries in years 2015 through 2021, generating 65 unique TSS-image combinations. Measured TSS values ranged from 1.4 to 216 mg L^{-1} (median 9.4 mg L^{-1}) and were collected between March 23 and November 1. LTMP samples are not collected in December, January, or February. Channel widths at the sampling point ranged from 17 to 117 m. Only one sample was collected at a time when the instantaneous discharge was greater than a 2-year recurrence interval flood (Olson, 2014), and 88% of the points were collected during the flood recession or when flows were relatively steady.

Overall, the single-band *Nechad* algorithm outperformed the multi-conditional *Novoa* algorithm (i.e., *Nechad* has a lower RMSLE and bias; Figure 2), but neither were highly accurate (i.e., ε=35-39%). For both algorithms, β was greater than zero indicating an over-prediction of TSS. Further exploration of the relationship between observed and estimated TSS values revealed that observed values less than ~50 mg L^{-1} are overestimated, but that there was a systematic bias for observed TSS values greater than ~50 mg L^{-1}, whereby the greater the observed value, the greater the under-prediction (Figure 3). To remove this systematic bias, we detrended the estimated-observed values based on the observed pattern to calculate the detrended percent error in the estimated TSS value relative to the observed value. We evaluated the absolute value of the percent error in estimated TSS. Because of the relatively similar results between the two algorithms, and the slightly better performance of *Nechad*, we limited the remainder of the analyses to the estimates provided by *Nechad*.

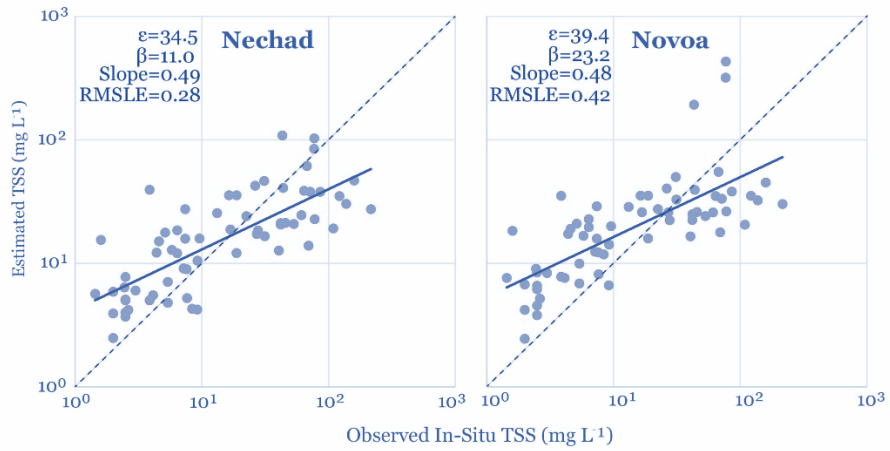

Figure 2. Observed vs estimated TSS values for the single (Nechad) and mutli-band (Novoa) algorithms

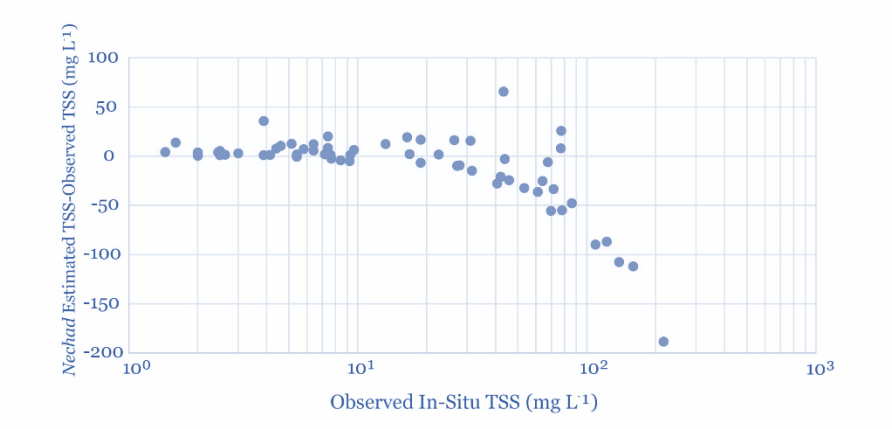

Figure 3. Difference between estimated and observed for Nechad demonstrating how the algorithm overpredicts TSS for values < ~50 mg L^{-1} and then systematically underpredicts TSS for observed values greater than ~50 mg L^{-1}

Percent error values for *Nechad* were not normally distributed, based on a Shapiro-Wilk test ($W=0.52$, $p<0.001$), and therefore we used the non-parametric Kruskal-Wallis method to evaluate differences in means and a post-hoc Dunn's Test (with a Bonferroni correction). Mean percent error was significantly greater for points located on wider rivers, for shallower flows, and when temperatures were warmer than 15 degrees (Table 2). The effects of the other factors (river flux, vegetation, hydrograph) on percent error were not significant (at $p<0.10$; Table 2). Strong associations (Cramer's V >0.60) existed within factor type (e.g., between factors that describe watershed setting, flow conditions, or season), and may explain unexpected results. River width was strongly associated with river flux grouping (Cramer's $V=0.67$). All low-flux rivers in our dataset are narrow and 75% of high-flux rivers are wide. Thus, while we expected wide channels to have lower errors, larger errors on wider channels may (in part) be a function of the character of the sediment load (i.e., mostly high flux settings).

Table 2. Comparison of mean % estimated error for the *Nechad* algorithm for the six factors tested

Factor	p-value	chi-squared	Category 1	n	mean error	Category 2	n	mean error
Flow Depth	0.01	7.1	shallow	25	1.32	deep	40	0.76
Channel Width	0.02	5.3	narrow	34	0.53	wide	31	1.46
Water Temperature	0.02	5.2	cold	29	0.81	warm	36	1.10
Vegetation	0.10	2.6	leaf off	18	0.52	leaf on	47	1.14
River Flux	0.21	1.6	high flux	43	1.21	low flux	22	0.51
Hydrograph	0.39	0.7	rising	8	1.94	falling/flat	57	0.84

Interactions between non-associated factors (Cramer's V <0.60) highlighted the mediating impact of water temperature on flow depths (Figure 4A and Table 3). Flow depth was a strong determinant of prediction errors, whereby TSS measurements collected during flows that are sufficiently deep have nearly half the error as those collected when flow depths were potentially not sufficient to prevent backscatter from the bed (Table 2). However, this effect only remained significant when water temperatures were < 15° C; for warmer water temperatures, errors were not significantly different between shallow and deep samples (Figure 4A), though we acknowledge a small sample size (n=3) for shallow-cold observations. Interactions also highlighted the importance of river flux, not apparent when considering single factors (Figure 4 and Table 3). Samples collected in high annual flux settings when leaves were on the trees had nearly 5 times greater error than those collected when leaves were off the trees (Figure 4B), and nearly double the error when flow depths were too shallow, but errors were similar on low-flux

rivers (Figure 4D). Similarly, water temperatures had an impact on prediction errors for high flux settings, and not for low flux settings; estimated TSS had nearly 4 times the prediction error for warm water in high flux settings than cold water (Figure 4C).

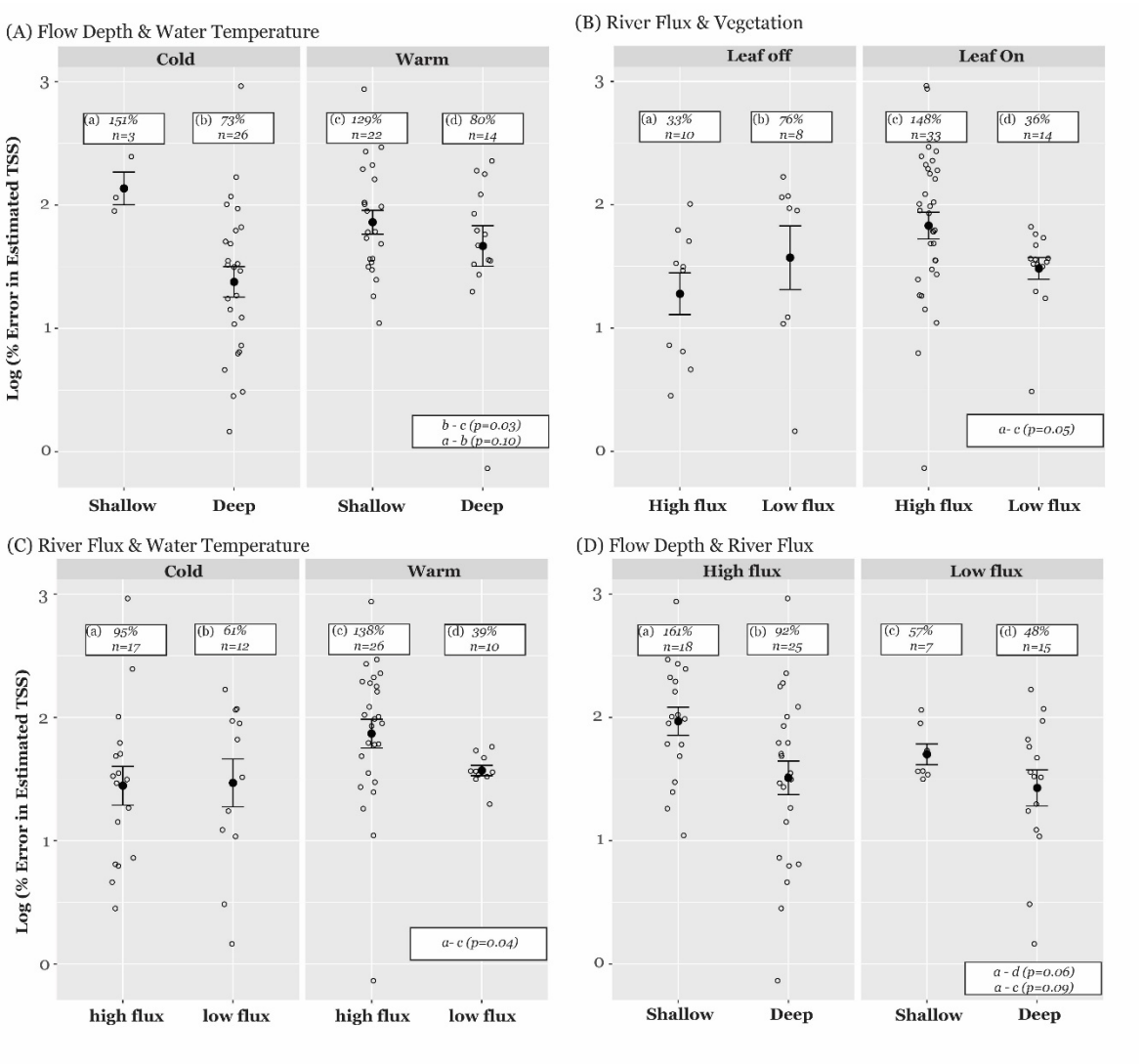

Figure 4. Four of the significant two-way interactions from Table 3 that highlight some of the mediating effects of one factor on another. Bars and black filled dot represent median and inter-quartile range. For each grouping, the average percent error is listed as well as the number of observations. Statistically different groupings are listed in the lower right-hand corner of each sub-panel.

Table 3. Differences in mean % estimated error for the *Nechad* algorithm considering two-way interactions of non-associated factors

Grouping	p-value	chi-squared
Flow Depth:Water Temperature	0.010	11.4
Flow Depth:River Width	0.010	11.3
River Flux:Vegetation	0.025	9.4
Channel Width: Water Temperature	0.025	9.4
River Flux: Water Temperature	0.030	8.9
Channel Width: Vegetation	0.033	8.8
Flow Depth:River Flux	0.038	8.4
Flow Depth:Vegetation	0.038	8.4
Hydrograph:Channel Width	0.045	8.0
Hydrograph:Water Temperature	0.078	6.8
Hydrograph:Vegetation	0.265	4.0
Hydrograph:River Flux	0.307	3.6

Discussion & Conclusion

Although broad-scale remote sensing applications are increasingly adopted into water quality assessments (Griffith, 2002), such applications are typically limited to larger rivers (e.g., Gardner et al., 2021), missing a large proportion of the river network (Downing et al., 2012). The motivation for this study was to assess the feasibility of moving such applications up the river network to smaller channels. We hypothesized that although spatially and temporally variable limitations exist, in certain watershed settings and under certain flow conditions and seasonal influences, there are opportunities to estimate TSS relying on remote sensing. To test the hypothesis we evaluated which factors described errors between estimated TSS values from widely-used algorithms and observed in-situ TSS values from an existing long-term dataset of "smaller" rivers (i.e., < 150 m). In our test bed of the Lake Champlain Basin, we found settings, and conditions, under which broad-scale remote sensing may be feasible. Additional evaluations using more explicit and larger datasets are still needed.

Flow depth was the strongest determinant of error in estimated TSS. When flows were "deep enough", errors were half of what they were on shallower rivers, no matter the width of the channel. Sufficient depths will vary from one river to the next depending on the concentration-discharge relationships for TSS. For the rivers in the Lake Champlain Basin, we found that the threshold between shallow and deep flows, based on the radiative transfer modeling of Legleiter et al. (2011) was ~80-90 cm. Seasonal characteristics also determined the successful application of remote sensing to smaller rivers. When water temperatures were warmer, which correlated with elevated chlorophyll-a levels, errors were ~40% greater than during times of the year when water temperatures were colder. During these warmer months leaves are also on trees interfering the near-bank signal along forested sites, and enhancing the organic matter in the water column, which can confound the relationship between surface reflectance and TSS (Martinez et al., 2015).

Temporally variable conditions were mediated by the watershed setting. Based on our dataset, wider rivers had higher errors in estimated TSS than narrower ones. This is counter-intuitive (e.g., Zhao et al., 2014) and possibly a function of the geography of the Lake Champlain Basin, whereby the wider rivers drain higher-relief catchments with greater mean annual precipitation and have higher annual sediment fluxes associated with coarser-grained sediments. This is in contrast with the three low-flux rivers in our dataset, which are all narrower than 50 meters, and

sourced directly from the Lake Champlain Valley, which is dominated by highly erodible, and very fine-grained glaciolacustrine deposits. Although these rivers are narrow, they have high background loads (i.e., sediment concentrations that are not sensitive to increasing discharge), and their loads are composed of finer grained particles. These finer-grained loads improve TSS estimates in two ways. First, the particles are more likely to be well mixed vertically than coarser particles, such that what is measured at depth (i.e., through depth-integrated sampling), is also representative of what is measured at the surface relying on surface reflectance values. Relatedly, fine particles distributed throughout the water column are likely to absorb more radiation, reducing the depths at which the bed influences the radiative signal. While river flux on its own was not a significant factor influencing error in estimated TSS, its importance as a mediating factor became evident when factor interactions were tested. For example, errors in estimated TSS were much higher when flows were shallow on high flux rivers (average of 161%), than on low flux rivers with either shallow (average of 57%) or deep (average of 48%) flows (Figure 4). Taken collectively, these findings suggest spatial and temporal conditions under which broad-scale remote sensing of TSS may be feasible in small rivers – namely, in nonvegetated, colder-water seasons at wash-load-dominated, narrow and deep channel settings.

Understanding where, and when, broad-scale remote sensing datasets may be applicable, may help to improve the efficiency and reach of watershed management plans targeting source areas for water quality impairments. Winter runoff events are challenging to sample, and often neglected by monitoring programs, yet recent evidence suggests that these events can have high turbidity and nutrient concentrations (Seybold et al., 2022). Winter runoff events are likely to increase with a warming climate (Contosta et al., 2019), and as such integrating remote-sensing based assessments into monitoring may help capture this increasingly important mechanism.

Because the geomorphology of rivers, their hydrologic regimes, and sediment transport characteristics vary greatly across topographic, geologic and hydroclimatic gradients, opportunities for remote-sensing based approaches on smaller rivers will be variable. For example, targeted flow depths of 80-90 cm, are associated with dramatically different discharges based on channel size and shape but also slope. While on larger rivers, or those that have a low width-to-depth ratio or low slopes, high exceedance flows (or those that occur most of the time) may be deep enough to prevent backscattering from the channel bed, whereas on smaller rivers and those that have a high width-to-depth ratio or high slopes, lower discharges are likely to interfere with reflectance. Rivers that drain erodible, fine-grained landscapes, such as those in the Lake Champlain Valley which flow through glaciolacustrine deposits, are likely to have high background loads, and transport sediment throughout the water column (Armijos et al., 2017). In contrast, rivers with a crystalline source-area lithology, for example, may transport coarser particles (e.g., sand) in suspension, which may be harder to measure in remotely-sensed imagery (Dethier et al., 2019). Additionally, where the growing season extends throughout the year, the opportunity for remote-sensing based TSS estimates may be more limited. Although in such settings, the consistency of organic material in the water column may contribute to the development of a more successful regional algorithm (Marinho et al., 2021).

We based our analyses on the errors in the application of *Nechad*, a single-band algorithm developed for open-water settings outside the region (Nechad et al., 2010), using a relatively small dataset curated from non-Winter, non-ice months in a temperate, glacially-conditioned setting. While single-band algorithms can be powerful tools, they often have limited applicability outside the region and the range of calibration values. Recently, Balasubramanian et al. (2020) and others have developed globally applicable tools, with great success, but these

tools have not been evaluated for smaller rivers. With the increasing availability of broad-scale, high-resolution satellite imagery (e.g., Frazier & Hemingway, 2021), there are growing opportunities to extend the reach of remote sensing-based watershed evaluations of water quality. Additional work is needed to define the conditions and settings under which broad scale remote sensing may be applied. Regional datasets and algorithms remain the most promising path forward, and further work is needed to develop robust algorithms on smaller rivers.

References

Alexander, R. B., Boyer, E. W., Smith, R. A., Schwarz, G. E., & Moore, R. B. (2007). The role of headwater streams in downstream water quality. *Journal of the American Water Resources Association*, *43*(1), 41–59. https://doi.org/10.1111/j.1752-1688.2007.00005.x

Armijos, E., Crave, A., Espinoza, R., Fraizy, P., Santos, A. L. M. R. D., Sampaio, F., de Oliveira, E., Santini, W., Martinez, J. M., Autin, P., Pantoja, N., Oliveira, M., & Filizola, N. (2017). Measuring and modeling vertical gradients in suspended sediments in the Solimões/Amazon River. *Hydrological Processes*, *31*(3), 654–667. https://doi.org/10.1002/hyp.11059

Balasubramanian, S. v., Pahlevan, N., Smith, B., Binding, C., Schalles, J., Loisel, H., Gurlin, D., Greb, S., Alikas, K., Randla, M., Bunkei, M., Moses, W., Nguyễn, H., Lehmann, M. K., O'Donnell, D., Ondrusek, M., Han, T. H., Fichot, C. G., Moore, T., & Boss, E. (2020). Robust algorithm for estimating total suspended solids (TSS) in inland and nearshore coastal waters. *Remote Sensing of Environment*, *246*. https://doi.org/10.1016/j.rse.2020.111768

Bi, N., Yang, Z., Wang, H., Fan, D., Sun, X., & Lei, K. (2011). Seasonal variation of suspended-sediment transport through the southern Bohai Strait. *Estuarine, Coastal and Shelf Science*, *93*(3), 239–247. https://doi.org/10.1016/j.ecss.2011.03.007

Contosta, A. R., Casson, N. J., Garlick, S., Nelson, S. J., Ayres, M. P., Burakowski, E. A., Campbell, J., Creed, I., Eimers, C., Evans, C., Fernandez, I., Fuss, C., Huntington, T., Patel, K., Sanders-DeMott, R., Son, K., Templer, P., & Thornbrugh, C. (2019). Northern forest winters have lost cold, snowy conditions that are important for ecosystems and human communities. *Ecological Applications*, *29*(7). https://doi.org/10.1002/eap.1974

Dethier, E., Renshaw, C. E., & Magilligan, F. J. (2019). Toward Improved Accuracy of Remote Sensing Approaches for Quantifying Suspended Sediment: Implications for Suspended-Sediment Monitoring. *Journal of Geophysical Research-Earth Surface*, *125*.

Downing, J. A., Cole, J. J., Duarte, C. M., Middelburg, J. J., Melack, J. M., Prairie, Y. T., Kortelainen, P., Striegl, R. G., McDowell, W. H., & Tranvik, L. J. (2012). Global abundance and size distribution of streams and rivers. *Inland Waters*, *2*(4), 229–236. https://doi.org/10.5268/IW-2.4.502

Fleming, P. M., Stephenson, K., Collick, A. S., & Easton, Z. M. (2022). Targeting for nonpoint source pollution reduction: A synthesis of lessons learned, remaining challenges, and emerging opportunities. *Journal of Environmental Management*, *308*, 114649.

Foley, J. A., DeFries, R., Asner, G. P., Barford, C., Bonan, G., Carpenter, S. R., Stuart Chapin, F., Coe, M. T., Daily, G. C., Gibbs, H. K., Helkowski, J. H., Holloway, T., Howard, E. A., Kucharik, C. J., Monfreda, C., Patz, J. A., Colin Prentice, I., Ramankutty, N., & Snyder, P. K.

(2005). Global Consequences of Land Use. *Science*, *309*, 570–574. https://www.science.org

Frazier, A. E., & Hemingway, B. L. (2021). A technical review of planet smallsat data: Practical considerations for processing and using planetscope imagery. *Remote Sensing*, *13*(19). https://doi.org/10.3390/rs13193930

Gardner, J. R., Yang, X., Topp, S. N., Ross, M. R. V., Altenau, E. H., & Pavelsky, T. M. (2021). The Color of Rivers. *Geophysical Research Letters* (Vol. 48, Issue 1). Blackwell Publishing Ltd. https://doi.org/10.1029/2020GL088946

Griffith, J. A. (2002). Geographic techniques and recent applications of remote sensing to landscape-water quality studies. *Water, Air, and Soil Pollution*, *138*, 181–197.

Kilham, N. E., Roberts, D., & Singer, M. B. (2012). Remote sensing of suspended sediment concentration during turbid flood conditions on the Feather River, California- a modeling approach. *Water Resources Research*, *48*(1). https://doi.org/10.1029/2011WR010391

Landers, M. N., & Sturm, T. W. (2013). Hysteresis in suspended sediment to turbidity relations due to changing particle size distributions. *Water Resources Research*, *49*(9), 5487–5500. https://doi.org/10.1002/wrcr.20394

Legleiter, C. J., Kinzel, P. J., & Overstreet, B. T. (2011). Evaluating the potential for remote bathymetric mapping of a turbid, sand-bed river: 1. Field spectroscopy and radiative transfer modeling. *Water Resources Research*, *47*(9). https://doi.org/10.1029/2011WR010591

Marinho, R. R., Harmel, T., Martinez, J. M., & Junior, N. P. F. (2021). Spatiotemporal dynamics of suspended sediments in the Negro River, Amazon Basin, from in situ and sentinel-2 remote sensing data. *ISPRS International Journal of Geo-Information*, *10*(2). https://doi.org/10.3390/ijgi10020086

Martinez, J. M., Espinoza-Villar, R., Armijos, E., & Silva Moreira, L. (2015a). The optical properties of river and floodplain waters in the Amazon River Basin: Implications for satellite-based measurements of suspended particulate matter. *Journal of Geophysical Research: Earth Surface*, *120*(7), 1274–1287. https://doi.org/10.1002/2014JF003404

Martinez, J. M., Espinoza-Villar, R., Armijos, E., & Silva Moreira, L. (2015b). The optical properties of river and floodplain waters in the Amazon River Basin: Implications for satellite-based measurements of suspended particulate matter. *Journal of Geophysical Research: Earth Surface*, *120*(7), 1274–1287. https://doi.org/10.1002/2014JF003404

Medalie, L. (2014). Concentration and Flux of Total and Dissolved Phosphorus, Total Nitrogen, Chloride, and Total Suspended Solids for Monitored Tributaries of Lake Champlain, 1990-2012. In *U.S. Geological Survey Open-File Report 2014-1209* (p. 21). http://dx.doi.org/10.3133/ofr20141209.

Murray, C., Larson, A., Goodwill, J., Wang, Y., Cardace, D., & Akanda, A. S. (2022). Water Quality Observations from Space: A Review of Critical Issues and Challenges. In *Environments - MDPI* (Vol. 9, Issue 10). MDPI. https://doi.org/10.3390/environments9100125

Nechad, B., Ruddick, K. G., & Park, Y. (2010). Calibration and validation of a generic multisensor algorithm for mapping of total suspended matter in turbid waters. *Remote Sensing of Environment*, *114*(4), 854–866. https://doi.org/10.1016/j.rse.2009.11.022

Novo, E. M., Hansom, J. D., & Curran, P. J. (1989). The effect of sediment type on the relationship between reflectance and suspended sediment concentration. *International Journal of Remote Sensing*, *10*(7), 1283–1289. https://doi.org/10.1080/01431168908903967

Novoa, S., Doxaran, D., Ody, A., Vanhellemont, Q., Lafon, V., Lubac, B., & Gernez, P. (2017). Atmospheric corrections and multi-conditional algorithm for multi-sensor remote sensing of suspended particulate matter in low-to-high turbidity levels coastal waters. *Remote Sensing*, *9*(1). https://doi.org/10.3390/rs9010061

NY State DEC, & VT DEC. (2020). *Long-term water quality and biological monitoring project for Lake Champlain 2018-2023. Quality Assurance Project Plan/workplan*. https://dec.vermont.gov/watershed/laes-onds/monitor/lake-champlain.

NY State DEC, & VT DEC. (2021). *Lake Champlain Long-Term Water Quality and Biological Monitoring Program. Project Description*. Lake Champlain Basin Program. https://dec.vermont.gov/watershed/laes-onds/monitor/lake-champlain.

NY State DEC, & VT DEC. (2022). *Lake Champlain Long-term Monitoring Tributary Data Set*. https://anrweb.vermont.gov/dec/_dec/LongTermMonitoringTributary.aspx

Ogle, D. H., Doll, J. C., Wheeler, P., & Dinno, A. (2022). *FSA: Fisheries Stock Analysis* (version 0.9.3).

Olmanson, L. G., Brezonik, P. L., & Bauer, M. E. (2013). Airborne hyperspectral remote sensing to assess spatial distribution of water quality characteristics in large rivers: The Mississippi River and its tributaries in Minnesota. *Remote Sensing of Environment*, *130*, 254–265. https://doi.org/10.1016/j.rse.2012.11.023

Olson, S. A. (2014). *Estimation of flood discharges at selected annual exceedance probabilities for unregulated, rural streams in Vermont* (p. 27). U.S. Geological Survey Scientific Investigations Report 2014-5078.

Pahlevan, N., Mangin, A., Balasubramanian, S. v., Smith, B., Alikas, K., Arai, K., Barbosa, C., Bélanger, S., Binding, C., Bresciani, M., Giardino, C., Gurlin, D., Fan, Y., Harmel, T., Hunter, P., Ishikaza, J., Kratzer, S., Lehmann, M. K., Ligi, M., … Warren, M. (2021). ACIX-Aqua: A global assessment of atmospheric correction methods for Landsat-8 and Sentinel-2 over lakes, rivers, and coastal waters. *Remote Sensing of Environment*, *258*. https://doi.org/10.1016/j.rse.2021.112366

Pahlevan, N., Smith, B., Alikas, K., Anstee, J., Barbosa, C., Binding, C., Bresciani, M., Cremella, B., Giardino, C., Gurlin, D., Fernandez, V., Jamet, C., Kangro, K., Lehmann, M. K., Loisel, H., Matsushita, B., Hà, N., Olmanson, L., Potvin, G., … Ruiz-Verdù, A. (2022). Simultaneous retrieval of selected optical water quality indicators from Landsat-8, Sentinel-2, and Sentinel-3. *Remote Sensing of Environment*, *270*. https://doi.org/10.1016/j.rse.2021.112860

R Core Team. (2022). *R: A language and environment for statistical computing*. R Foundation for Statistical Computing. https://www.R-project.org/.

Scott, D. T., Gomez-Velez, J. D., Jones, C. N., & Harvey, J. W. (2019). Floodplain inundation spectrum across the United States. *Nature Communications*, *10*(1), 5194. https://doi.org/10.1038/s41467-019-13184-4

Seybold, E. C., Dwivedi, R., Musselman, K. N., Kincaid, D. W., Schroth, A. W., Classen, A. T., Perdrial, J. N., & Adair, E. C. (2022). Winter runoff events pose an unquantified continental-scale risk of high wintertime nutrient export. *Environmental Research Letters*, *17*(10). https://doi.org/10.1088/1748-9326/ac8be5

Smeltzer, E., Shambaugh, A. d., & Stangel, P. (2012). Environmental change in Lake Champlain revealed by long-term monitoring. *Journal of Great Lakes Research*, *38*(SUPPL. 1), 6–18. https://doi.org/10.1016/J.JGLR.2012.01.002

Smith, B., Pahlevan, N., Schalles, J., Ruberg, S., Errera, R., Ma, R., Giardino, C., Bresciani, M., Barbosa, C., Moore, T., Fernandez, V., Alikas, K., & Kangro, K. (2021). A Chlorophyll-a Algorithm for Landsat-8 Based on Mixture Density Networks. *Frontiers in Remote Sensing*, *1*. https://doi.org/10.3389/frsen.2020.623678

Stanley, E. H., Collins, S. M., Lottig, N. R., Oliver, S. K., Webster, K. E., Cheruvelil, K. S., & Soranno, P. A. (2019). Biases in lake water quality sampling and implications for macroscale research. *Limnology and Oceanography*, *64*(4), 1572–1585. https://doi.org/10.1002/lno.11136

Topp, S. N., Pavelsky, T. M., Jensen, D., Simard, M., & Ross, M. R. V. (2020). Research trends in the use of remote sensing for inland water quality science: Moving towards multidisciplinary applications. *Water (Switzerland)* (Vol. 12, Issue 1). MDPI AG. https://doi.org/10.3390/w12010169

Underwood, K. L., Rizzo, D. M., Schroth, A. W., & Dewoolkar, M. M. (2017). Evaluating spatial variability in sediment and phosphorus concentration-discharge relationships using Bayesian inference and self-organizing maps. *Water Resources Research*, *53*, 293–316. https://doi.org/10.1002/2017WR021353

Vanhellemont, Q., & Ruddick, K. (2016). ACOLITE for Sentinel-2: Aquatic applications of MSI imagery. *ESA Special Publication SP*. https://odnature.naturalsciences.be/remsem/acolite-

Volpe, V., Silvestri, S., & Marani, M. (2011). Remote sensing retrieval of suspended sediment concentration in shallow waters. *Remote Sensing of Environment*, *115*(1), 44–54. https://doi.org/10.1016/j.rse.2010.07.013

Wohl, E. (2017). The significance of small streams. *Frontiers in Earth Science*, *11*(3), 447–456. https://doi.org/10.1007/s11707-017-0647-y

Zhao, D., Lv, M., Zou, X., Wang, P., Yang, T., & An, S. (2014). What is the minimum river width for the estimation of water clarity using medium-resolution remote sensing images? *Water Resources Research*, *50*(5), 3764–3775. https://doi.org/10.1002/2013WR015068